ML-Assisted Optimal Power and GSNR Estimation in Multi-band Elastic Optical Networks

N.B. When citing this work, cite the original published paper.

(article starts on next page)

ML-Assisted Optimal Power and GSNR Estimation in Multi-band Elastic Optical Networks

K. Ghodsifar[1], F. Arpanaei[2*], H. Beyranvand[1], M. Ranjbar Zefreh [3], C. Natalino[4], P. Monti[4], S. Yan[5], Ó. González de Dios[6], J. M. Rivas-Moscoso[6] J. P. Fernández-Palacios[6], A. Sánchez-Macián[2], D. Larrabeiti[2], and J. A. Hernández[2]

[1]*Dep. of Electrical Engineering, Amirkabir University of Technology, Tehran, Iran, [2]Dep. of Telematic Engineering, Universidad Carlos III de Madrid, Leganes, Madrid, Spain. [3]CISCO Systems S.R.L., Vimercate (MB), Italy. [4]Dep. of Electrical Engineering, Chalmers University of Technology, Gothenburg, Sweden, [5]Dep. Electrical Engineering, University of Bristol, Bristol, UK, [6]Telefónica Global CTIO, S/N, Madrid, Spain.*

*farhad.arpanaei@uc3m.es

ABSTRACT

A significant challenge in next-generation intelligent and autonomous optical networks is the rapid estimation of quality of transmission (QoT), particularly in multi-band and low-margin systems. These systems pose additional complexities, primarily stemming from inter-channel stimulated Raman scattering, which affects the gain-loss power and generalized signal-to-noise ratio (GSNR) profiles. GSNR profile calculation depends on various factors, including the loading state of the links, modulation format, launch power, and channels' bandwidth. These complexities contribute to the time-consuming nature of estimating QoT in such systems. This study employs a semi-closed form model (CFM) based on the (enhanced) Gaussian noise (GN/EGN) analytical equations to estimate the GSNR, generating datasets. Machine learning (ML) models are then trained using these datasets to accurately estimate optical power and GSNR profiles, achieving errors below 0.04 dB for power and 0.1 dB for GSNR in 99% of cases. The use of ML models is justified by their computational efficiency, aiding in online network management. We adopt the ML models in a power optimization algorithm that maximizes network total capacity. The power optimization using the ML models take 25-50 times lower time, while resulting in a maximum of 0.1 dBm error versus the analytical semi-CFM.
Keywords: Elastic Optical Networks; Multi-band; Deep Neural Network; Power Optimization.

1. INTRODUCTION

The most daunting aspect of GSNR estimation for multi-band elastic optical networks (MB-EONs) revolves around accurately estimating non-linear interference (NLI) power and amplified spontaneous emission (ASE) power, where the inter-channel stimulated Raman scattering effects exert significant influence. However, while NLI models in the time-frequency domain boast high accuracy, they rely on solving intricate integrals, rendering them impractical for online or offline network planning tools [1]. Models like the split-step Fourier method and integral-based GN/EGN model demand excessive computational time [2]. Moreover, their complexity limits their ability to adequately address add/drop effects modeling in network-wide studies. Consequently, over recent years, researchers have developed several CFMs (e.g., [3]) and semi-CFMs (e.g., [4, 5]) to estimate NLI. While CFMs offer closed-form formulas for power evolution profile and NLI, they rely on specific assumptions, potentially compromising accuracy if the system model deviates from these assumptions. Semi-CFMs calculate power evolution profile and loss coefficients using fitting approaches, providing flexibility to bypass certain assumptions. The generalized GN model (GGN), widely used in dense wavelength-division multiplexing (DWDM) systems, lacks modulation format correction terms crucial for MB-EONs [6]. Recently, four fast CFMs have emerged, as discussed in [3, 7–9]. The model proposed in [3] exhibits superior accuracy for LCS1-band scenarios, especially with additional correction forms, albeit primarily focusing on Gaussian-shaped signals. Conversely, [9] introduced a CFM considering Raman windowing across the frequency axis to enhance accuracy, particularly for L+C-band scenarios. Notably, semi-CFMs introduced in [4, 5] offer adequate accuracy for EONs beyond the C+L+S1-band. Due to the high complexity of models like GGN and semi-CFM, the ASE-shaped noise loading approach is often employed for idle channel ASE noise loading to maintain a consistent optimum power profile, thus circumventing the need for GSNR calculation by altering the power profile of each link. However, in real networks, this approach leads to increased energy consumption.

In our study, we propose ML-assisted QoT estimation models for power and GSNR estimation, achieving computation times 25-50 times faster than analytical semi-CFM. We apply these for finding the power profile per span, achieving a maximum error of 0.1 dBm. Consequently, the addition of ASE-shaped noise loading becomes unnecessary in next-generation MB-EONs, allowing for the estimation of GSNR for affected channels within a few seconds.

Table 1: Features for ML-assisted power estimation models

No.	Parameter
1	Span length
2	Channel launch power
3	Total launch power of all channels
4	Channel position
5	Percentage of activity of all channels
6	Percentage of activity of channels to the left of the channel under test
7	Percentage of activity of channels to the right of the channel under test
8	Idle channels to the left of the channel under test
9	Idle channels to the right of the channel under test
10	Percentage of activity of the first quarter channels
11	Percentage of activity of the second quarter channels
12	Percentage of activity of the third quarter channels
13	Percentage of activity of the fourth quarter channels

Table 2: Features for ML-assisted GSNR estimation models

Item	Description
1-13	Features 1-13 in Table 1
14	Modulation format used in the channel
15	Maximum modulation formats used
16	Minimum modulation formats used
17	Average modulation formats used
18	Standard deviation of modulation formats used
19	Channel power at the end of the span

2. DATASETS GENERATION

To generate the synthesized datesets, we utilize the advanced ML-based GN/EGN model from [4, 10], which has been validated through both the split-step Fourier method and experimental testing [11]. This model incorporates essential features such as dispersion and modulation format correction terms, ensuring a balance between accuracy and speed in estimating GSNR for each span, following methodologies outlined and utilizing equations (1)-(6) in [10]. Since the trained ML model should be able to provide QoT estimations in different scenarios, it needs to be exposed to a wide range of network configurations, and trained accordingly. Therefore, a dataset based on diverse conditions and random parameters has been created. Four primary features are taken into account to generate the scenarios, including span length, loading factor (percentage of activity of each band), modulation format of each channel, and launch power. Each scenario is characterized by these four features. This is in contrast to previous studies [12] and [13], where authors generated biased datasets, the synthesized datasets in this work are topology independent.

3. ML-ASSISTED METHODOLOGIES AND ALGORITHMS

Two ML-assisted methods are proposed for power and GSNR estimation. Both methods utilize two powerful and well-known ML models, namely gradient boosting (GB) and neural network (NN). Regarding the power estimation, the power at the end of each span can be estimated using the proposed ML model, replacing the time-consuming solution of coupled differential Raman equations, particularly burdensome for MB-EONs. For GSNR estimation, we estimate the GSNR of each span using the three proposed ML models instead of relying on the time-consuming semi-CFM. The features for power and GSNR estimation are listed in Tables 1 and 2, respectively. Additionally, the GB, and two NNs with different architectures (with 1 and 2 hidden layers respectively) are considered as ML models.
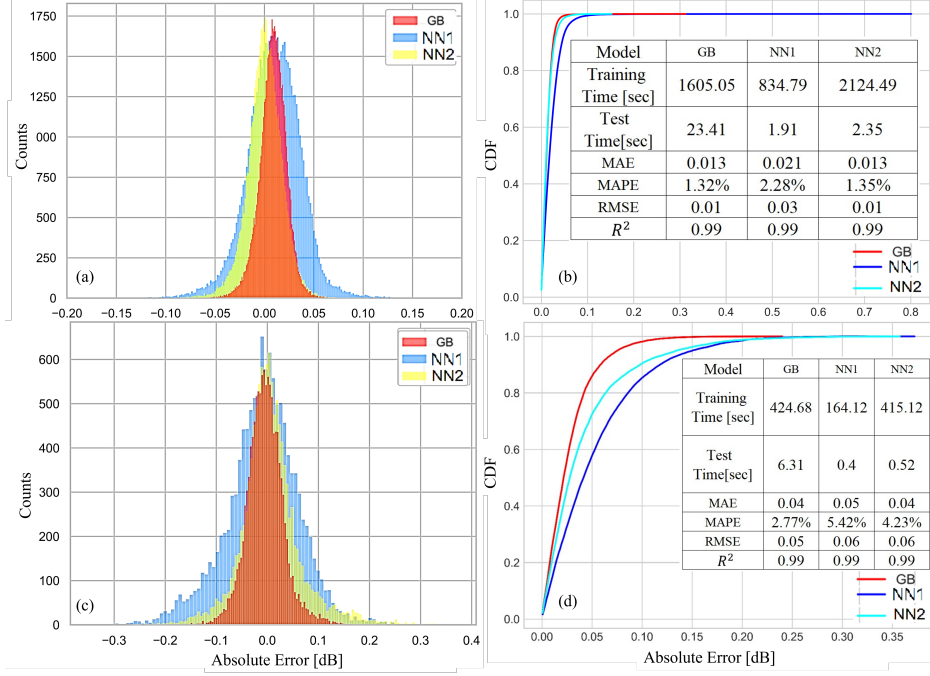
Fig. 1: Histogram of the power (a) and GSNR (c) absolute error for different gradient boosting (GB), neural network 1 (NN1), and neural network 2 (NN2) models. Cumulative distribution function (CDF) of the power (b) and GSNR (d) absolute error for GB, NN1, and NN2 models, along with the corresponding KPIs and training and test times.

4. Simulation Results, Discussions, and Conclusions

Based on the system model discussed later, four key features – span length, launch power, loading factor, and modulation format cardinality – are chosen within specific ranges, typical for metro-core backbone networks. These ranges are set as follows: [40, 100] km with a granularity of 10 km for span length, [-5, 5] dBm with a granularity of 0.1 dBm for launch power, [50%, 100%] with a granularity of 10% for loading factor, and [1, 6] for modulation format cardinality. For simplicity, we consider the C+L-band with 12 (6+6) THz, although the proposed model can extend beyond this range. We use a symbol rate of 64 GBaud, a roll-off factor of 0.05, and assume standard single-mode fiber with zero water peak characteristics to adjust the loss, dispersion, nonlinear coefficients, effective area, and refraction coefficient. Each span consists of 160×75 GHz channels, with 400 GHz between the C and L bands. Initially, we generate 2,500 scenarios (spans) based on different values of the main features, resulting in 400,000 ($2,500 \times 160$) samples, of which 300,700 are non-idle. We allocate 80% of the dataset for training, 20% for testing, and 20% of the training set for validation using 5-fold cross-validation to determine optimum hyperparameters.

In both the power and GSNR estimation models, the hyperparameters for the GB model include a sub-sample of 0.1, a learning rate of 0.01, a maximum depth of 10, and 15×10^3 estimators. In the GSNR NN models use Relu activation function. NN1 has one layer with 500 neurons, while NN2 has two layers with 500 neurons each. In the power estimation models, the NN1 comprises one layer with 1000 neurons and Tanh as the activation function, while the NN2 consists of two layers with 500 neurons each with Relu as the activation function. In all models, a mean absolute error (MAE) loss function is utilized, and training is performed using the Adamax optimizer for 150 epochs. The histogram of the absolute error for both power and GSNR is illustrated in Fig. 1 (a) and (c), respectively. The results show that the GB model achieves the highest accuracy among the three. Four key performance indicators (KPIs) are considered to compare the performance of ML models, including mean absolute error (MAE), mean absolute percentage error (MAPE), root mean square error (RMSE), and R^2. All KPIs indicate that the GB model is the most accurate. However, the run-time results reveal an inverse relationship between accuracy and run-time, with the GB model being the most accurate yet time-consuming. Regarding training run-time, the NN1 exhibits lower accuracy but faster training time. Conversely, both the NN2 and GB models demonstrate the same accuracy, but the GB model offers faster training time. Furthermore, for both power and GSNR estimation, the cumulative distribution function of the GB

Table 3: Optimal Power in [dBm] and run-time in [sec] for different span lengths and analytical and ML-based models.

Span Length [km]	Analytical (dBm, sec)	GB (dBm, sec)	NN1 (dBm, sec)	NN2 (dBm, sec)
50	(-1.4, 18.82)	(-1.4, 0.99)	(-1.4, 0.71)	(-1.5, 0.71)
60	(-0.7, 39.91)	(-0.8, 1.73)	(-0.8, 1.13)	(-0.8, 1.17)
70	(-0.1, 62.61)	(-0.2, 2.46)	(-0.2, 1.58)	(-0.2, 1.66)
80	(0.5, 89.95)	(0.4, 3.22)	(0.4, 2.05)	(0.4, 2.23)
90	(1.0, 118.56)	(1.0, 3.96)	(1.0, 2.53)	(0.9, 2.56)
100	(1.5, 150.94)	(1.5, 4.57)	(1.5, 2.92)	(1.5, 3.03)

model indicates that 99% of samples have less than 0.1 dB error. Moreover, while the accuracy of the NN2 model may not match that of the GB model for GSNR estimation, their run times exhibit a similar trend, as demonstrated in the power estimation models. Finally, based on the same approach of power optimization proposed in [14], two approaches based on the analytical semi-CFM and ML-assisted model are compared. As observed in Table 3, the power found by all three machine learning models has a maximum error of 0.1 dBm. The significant issue is the execution time. Among the three machine learning models, as observed in previous tests, the fastest model is NN1, and the slowest is GB. However, the execution time of the algorithm in these results using ML models will be approximately 25-50 times faster than the analytical method. Therefore, using ML methods with a maximum error of 0.1 dBm, near-optimal power can be found within a maximum of 25 times lower the execution time of the analytical method.

ACKNOWLEDGEMENTS

References

1. P. Poggiolini, G. Bosco, A. Carena, V. Curri, Y. Jiang, and F. Forghieri. The GN-model of fiber non-linear propagation and its applications. *Journal of Lightwave Technology*, 32(4):694–721, 2014.
2. P. Poggiolini and Y. Jiang. Recent advances in the modeling of the impact of nonlinear fiber propagation effects on uncompensated coherent transmission systems. *Journal of Lightwave Technology*, 35(3):458–480, 2017.
3. Daniel Semrau, Eric Sillekens, Robert I. Killey, and Polina Bayvel. A modulation format correction formula for the Gaussian noise model in the presence of inter-channel stimulated raman scattering. *Journal of Lightwave Technology*, 37(19):5122–5131, 2019.
4. Mahdi Ranjbar Zefreh and Pierluigi Poggiolini. A real-time closed-form model for nonlinearity modeling in ultra-wide-band optical fiber links accounting for inter-channel stimulated raman scattering and co-propagating raman amplification. *2020, arXiv:2006.03088,[eess.SP]*.
5. H. Buglia, M. Jarmolovičius, A. Vasylchenkova, E. Sillekens, L. Galdino, R. I. Killey, and P. Bayvel. A closed-form expression for the gaussian noise model in the presence of inter-channel stimulated raman scattering extended for arbitrary loss and fibre length. *Journal of Lightwave Technology*, 41(11):3577–3586, 2023.
6. Andrea D'Amico, Bruno Correia, Elliot London, Emanuele Virgillito, Giacomo Borraccini, Antonio Napoli, and Vittorio Curri. Scalable and disaggregated ggn approximation applied to a c+ l+ s optical network. *Journal of Lightwave Technology*, 40(11):3499–3511, 2022.
7. Dimitris Uzunidis, Evangelos Kosmatos, Chris Matrakidis, Alexandros Stavdas, and Andrew Lord. Strategies for upgrading an operator's backbone network beyond the C-band: Towards multi-band optical networks. *IEEE Photonics Journal*, 13(2):1–18, 2021.
8. Andre Souza, Nelson Costa, Joao Pedro, and Joao Pires. Comparison of fast quality of transmission estimation methods for CLS optical systems. *Journal of Optical Communications and Networking*, 15(11):F1–F12, 2023.
9. Chiara Lasagni, Paolo Serena, Alberto Bononi, and Jean-Christophe Antona. A generalized Raman scattering model for real-time SNR estimation of multi-band systems. *Journal of Lightwave Technology*, 41(11):3407–3416, 2023.
10. Pierluigi Poggiolini and Mahdi Ranjbar-Zefreh. Closed form expressions of the nonlinear interference for UWB systems. In *European Conference on Optical Communication (ECOC)*, page Tu1D.1, 2022.
11. Yanchao Jiang, Antonino Nespola, Alberto Tanzi, Stefano Piciaccia, Mahdi Ranjbar Zefreh, Fabrizio Forghieri, and Pierluigi Poggiolini. Experimental test of a UWB closed-form EGN model. In *European Conference on Optical Communications (ECOC)*, pages 254–257, 2023.
12. Ann Margareth Rosa Brusin, Antonino Nespola, Mahdi Ranjbar Zefreh, Stefano Piciaccia, Pierluigi Poggiolini, Fabrizio Forghieri, and Andrea Carena. ML-based spectral power profiles prediction in presence of ISRS for ultra-wideband transmission. *Journal of Lightwave Technology*, 42(1):37–47, 2024.
13. Yao Zhang, Min Zhang, Yuchen Song, Yan Shi, Chunyu Zhang, Cheng Ju, Bingli Guo, Shanguo Huang, and Danshi Wang. Building a digital twin for large-scale and dynamic C+L-band optical networks. *Journal of Optical Communications and Networking*, 15(12):985–998, 2023.
14. Farhad Arpanaei et al. Hyperaccelerated power optimization in multi-band elastic optical networks. In *Optical Fiber Communications Conference and Exhibition (OFC)*, page Th1I.6, 2024.